

Supporting Information

High performance functionalized anthracene organic supercapacitors

Sudipta Biswas, Rajendran Manikandan, Nitzan Shauloff, Shubhra Kanti Bhaumik, Raz Jelinek*

S. Biswas, R. Manikandan, N. Shauloff, S. K. Bhaumik, R. Jelinek.

Department of Chemistry

Ben Gurion University of the Negev

Beer Sheva 8410501, Israel

*E-mail: razi@bgu.ac.il

R. Jelinek.

Ilse Katz Institute for Nanotechnology

Ben Gurion University of the Negev

Beer Sheva 8410501, Israel

Keywords: Anthracene, polyaniline, organic supercapacitors, pseudo-capacitance, polyaniline

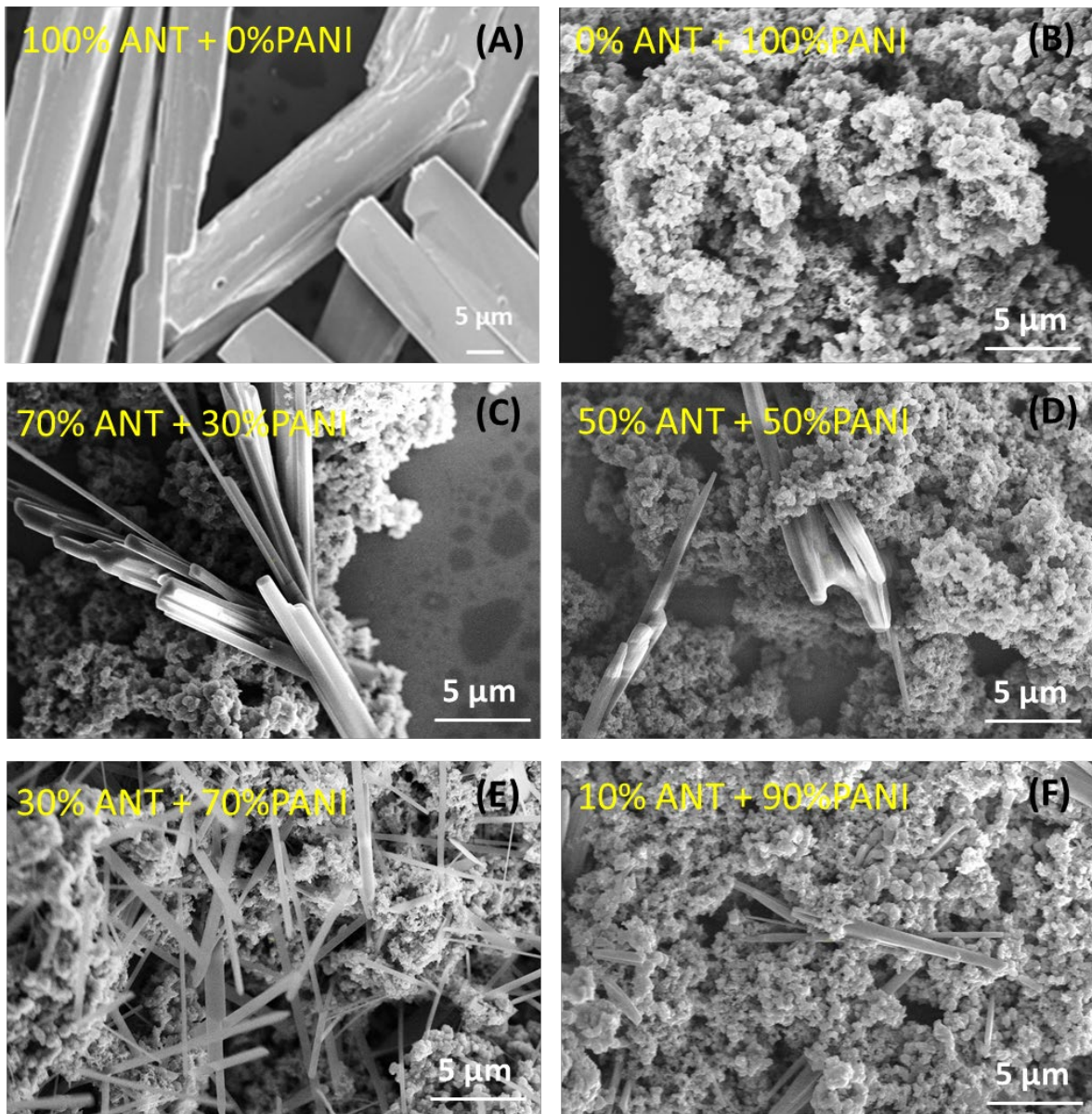
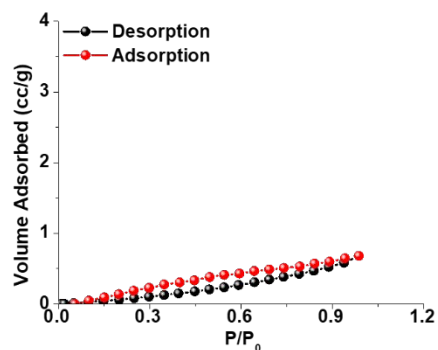
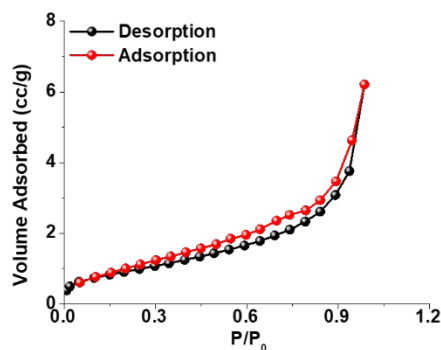


Figure S1 SEM micrographs for A. Pristine *tert*-butyl-ethylene-ketone-ANT, B. PANI, and C-F. Pristine *tert*-butyl-ethylene-ketone-ANT/PANI composite with varying weight ratios.

tert-butyl-ethylene-ketone-Anthracene



Polyaniline



tert-butyl-ethylene-ketone-Anthracene 30 wt% + polyaniline 70 wt%

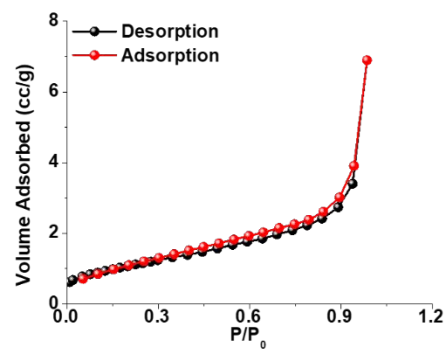


Figure S2 N₂ adsorption desorption curve for tert-butyl-ethylene-ketone-Anthracene (Surface area: 16.9 m²/g), polyaniline (Surface area: 36.5 m²/g) and tert-butyl-ethylene-ketone-Anthracene/polyaniline composite (3:7) (Surface area: 43.6 m²/g).

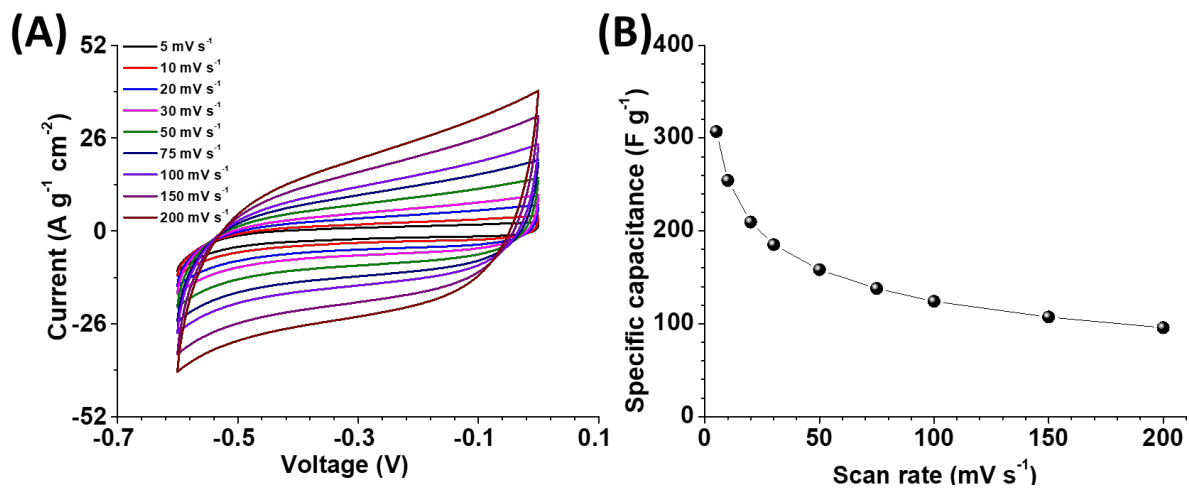


Figure S3 A. CV curves for electrode prepared using RGO/AC composite (1:1 weight ratio). B.

Corresponding specific capacitance calculated from each of the CV at various scan rate.

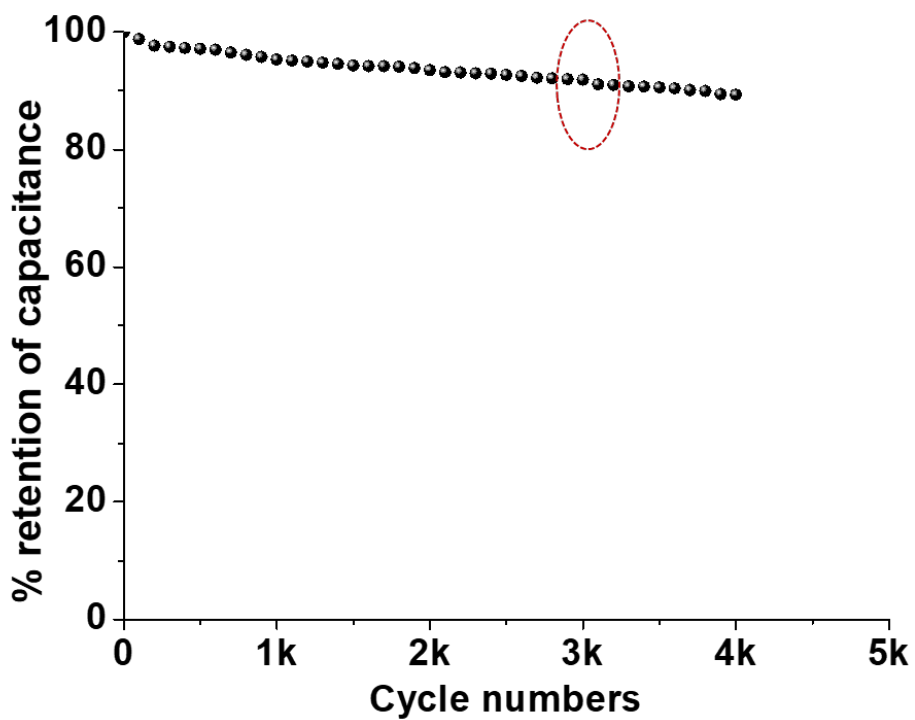


Figure S4. Cycling a fresh device to 3000 cycles followed by a 72 hrs resting and then a final 1000 cycles. After resting only, a 0.6% drop in capacitance is observed.

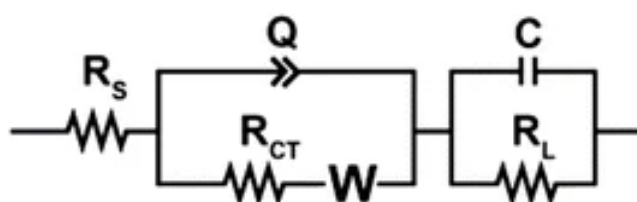


Figure S5 Equivalent series circuit to fit the EIS measured for aqueous device.

NMR spectra were recorded on Bruker DPX 400 instruments. The Chemical shifts, given in ppm, are relative to the residual solvent peaks.

Spectral data for the anthracene derivatives.

ketone-ANT: Following the general procedure **1**, the product **methyl-ethylene-ketone-ANT** was obtained as a pale yellow solid and the structure of the compound was confirmed by ¹H and ¹³CNMR data with those reported in previous literature.¹

¹H NMR (400 MHz, CDCl₃): δ 8.49 (d, *J* = 15.6 Hz, 1H), 8.47 (s, 1H), 8.21 (dd, *J* = 7.6, 3.8 Hz, 2H), 8.03 (dd, *J* = 7.6, 3.8 Hz, 2H), 7.54 – 7.47 (m, 4H), 6.72 (d, *J* = 15.6 Hz, 1H), 2.57 (s, 3H).

¹³C NMR (100 MHz, CDCl₃): δ 197.8, 140.6, 136.0, 131.4, 129.5, 129.1, 128.6, 126.6, 125.6, 125.2, 28.2.

HRMS (ESI): calc. for [(C₁₈H₁₄O)H] (M+H) 247.1123, measured 247.1113.

tert-butyl-ethylene-ketone-ANT: Following the general procedure **1**, the product **tert-butyl-ethylene-ketone-ANT** was obtained as a pale yellow solid and the structure of the compound was confirmed by ¹H and ¹³CNMR data with those reported in previous literature.¹

¹H NMR (400 MHz, CDCl₃): δ 8.63 (d, *J* = 15.6 Hz, 1H), 8.46 (s, 1H), 8.22 (dd, *J* = 7.6, 3.8 Hz, 2H), 8.06 (dd, *J* = 7.6, 3.8 Hz, 2H), 7.52 – 7.49 (m, 4H), 7.10 (d, *J* = 15.6 Hz, 1H), 1.30 (s, 9H).

HRMS (ESI): calc. for [(C₂₁H₂₀O)H] (M+H) 288.1514, measured 288.1509.

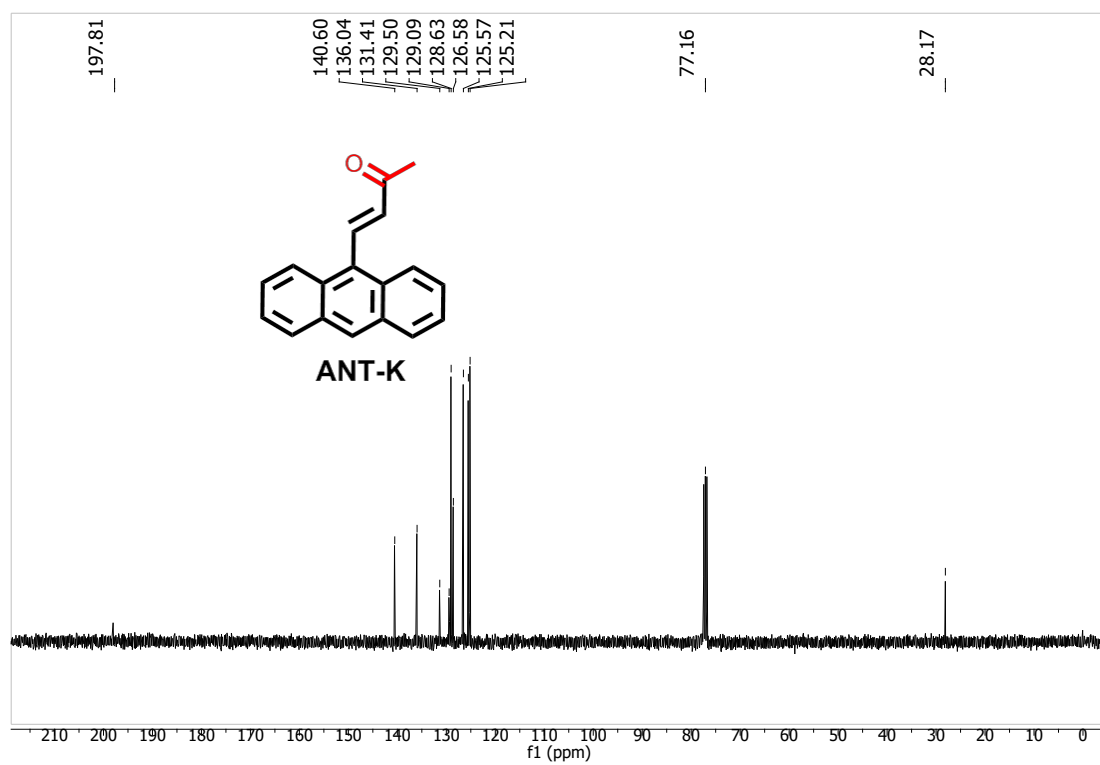
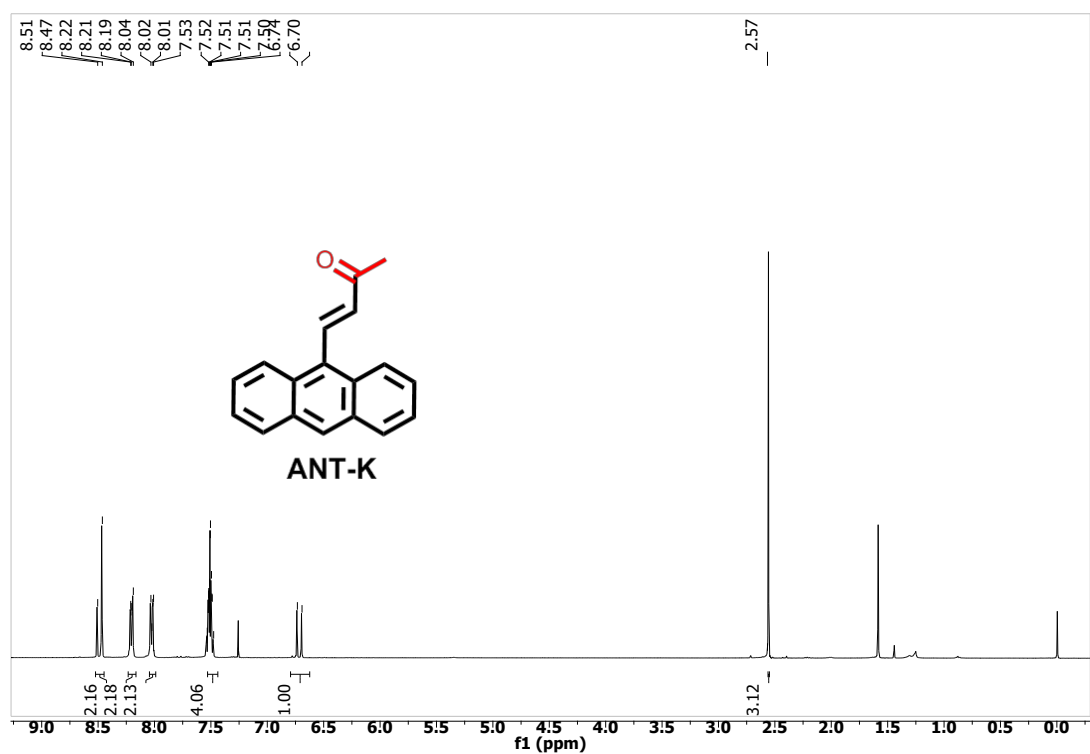
cyano-ethylene-ANT: Following the general procedure **2**, the product **cyano-ethylene-ANT** was obtained as an orange solid and the structure of the compound was confirmed by ¹H and ¹³CNMR data with those reported in previous literature.¹

¹H NMR (400 MHz, CDCl₃): δ 8.96 (s, 1H), 8.66 (s, 1H), 8.10 (d, *J* = 15.6 Hz, 2H), 7.94 (d, *J* = 15.6 Hz, 2H) (dd, *J* = 7.6, 3.8 Hz, 2H), 7.70 – 7.66 (m, 2H), 7.61 – 7.57 (m, 2H).

¹³C NMR (100 MHz, CDCl₃): δ 160.7, 132.6, 131.0, 129.7, 129.2, 128.5, 126.2, 124.0, 113.0, 111.3.

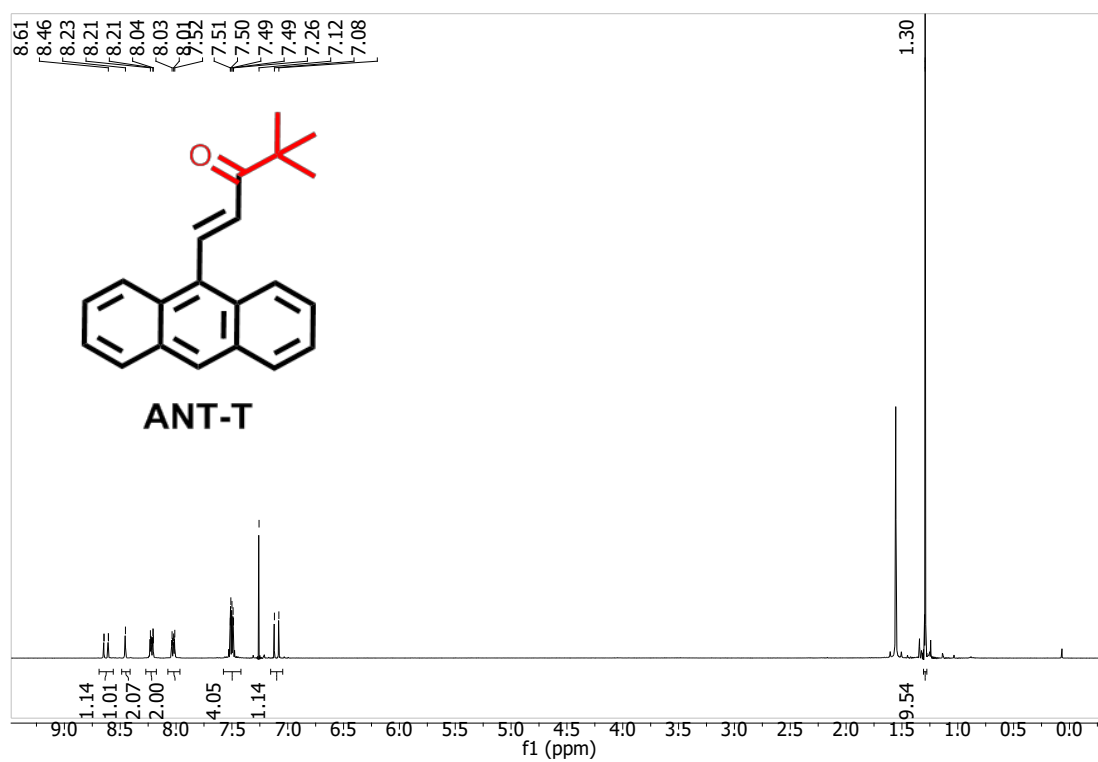
HRMS (ESI): calc. for $[(C_{18}H_{11}N_2)H]$ (M+2H) 256.1000, measured 256.2632.

Figure S6: 1H and ^{13}C NMR Spectra of methyl-ethylene-ketone-ANT



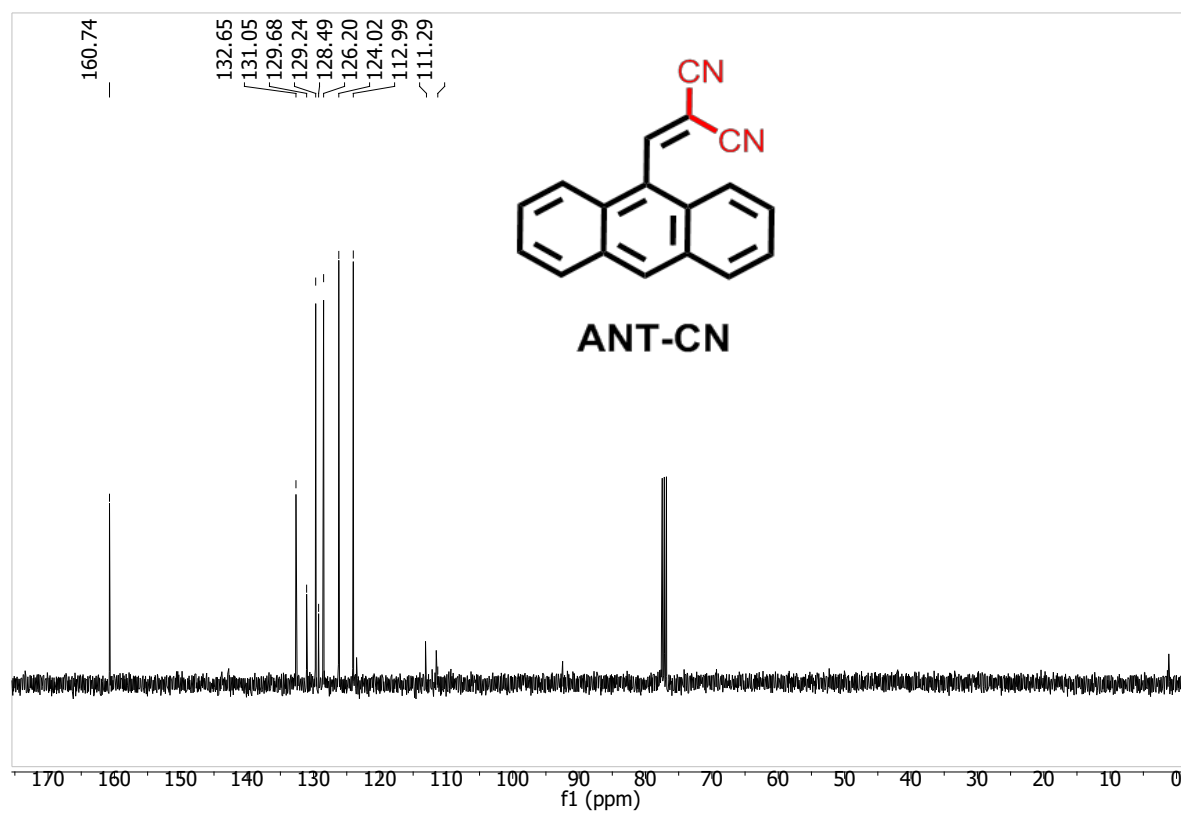
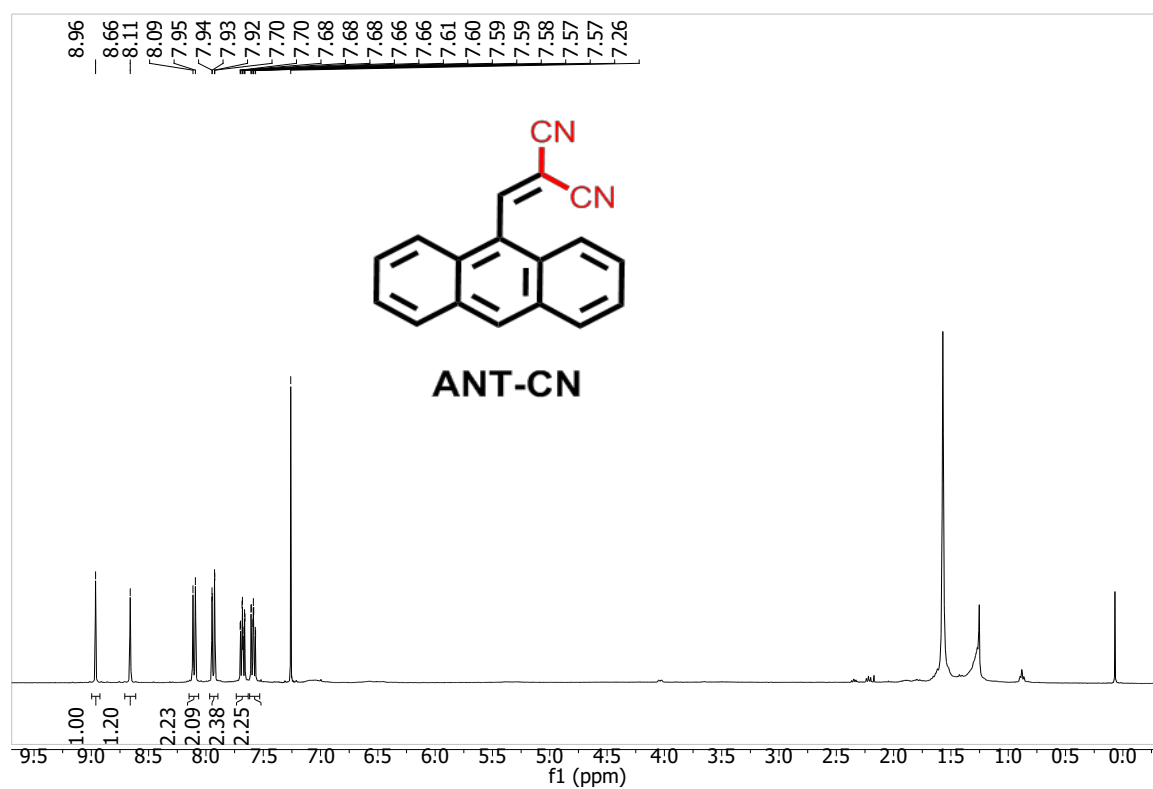
Chemical shift (ppm)

Figure S7: ^1H and ^{13}C NMR Spectra of *tert*-butyl-ethylene-ketone-ANT



Chemical shift (ppm)

Figure S8: ^1H and ^{13}C NMR spectra of cyano-ANT



Chemical shift (ppm)

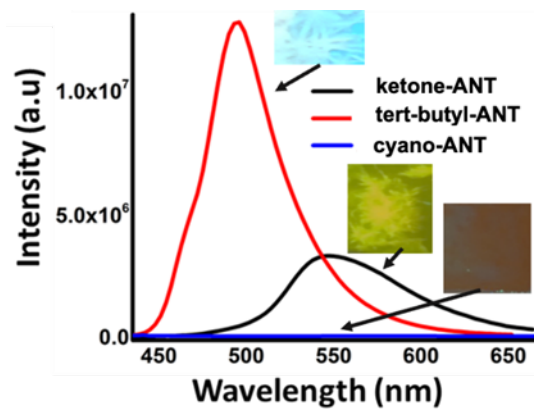


Figure S9. PL spectra of deposited anthracene derivatives on glass slides using ethanol (insets showing glass coated with material under UV). Fluorescence spectroscopy measurements were carried out using a Fluorolog spectrophotometer (HORIBA Scientific, Irvine, CA) (Shown in Figure S7).

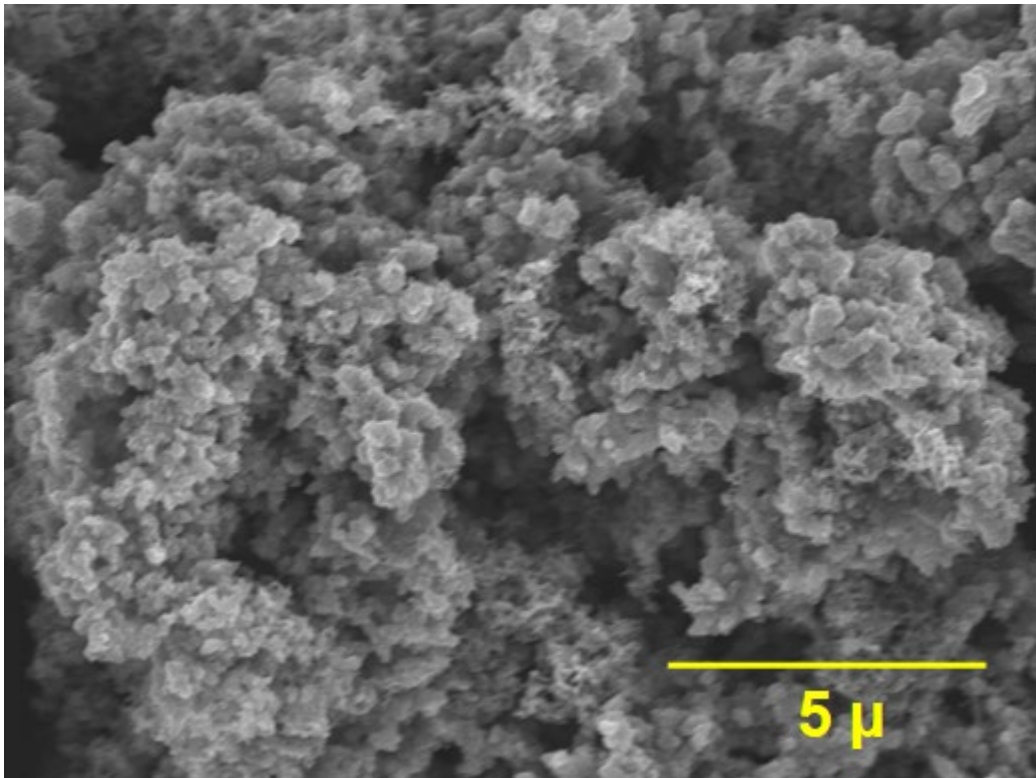


Figure S10. SEM micrograph of Polyaniline.

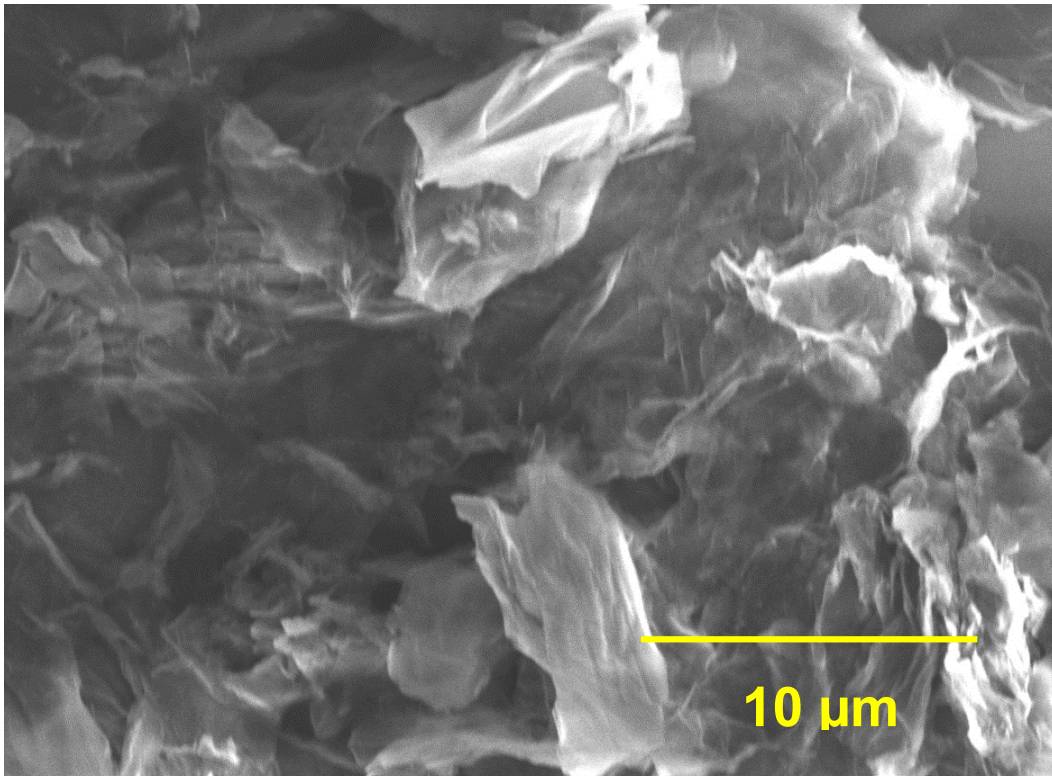


Figure S11. SEM micrograph of reduced graphene oxide.

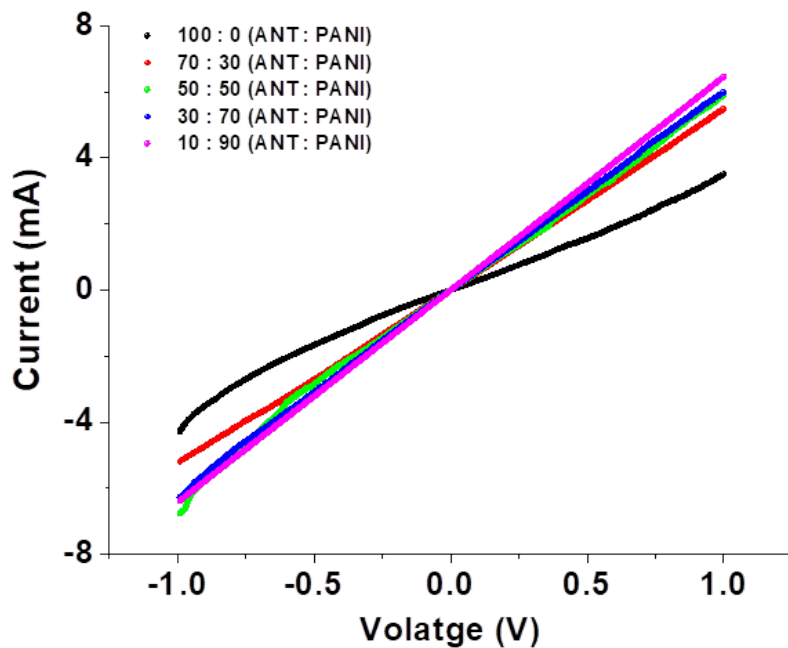


Figure S12. IV characteristic of composites with varying concentration of PANI and slope indicate with PANI, conductivity increases.

Conductivity of the *tert*-butyl-ethylene-ketone-ANT/PANI thin films (2 cm length).

ANT with PANI	Pure ANT	30% PANI	50% PANI	70% PANI	90% PANI
Material conductivity ($\Omega^{-1} \text{ cm}$) $\times 10^{-3}$	3.56	5.50	5.58	6.00	6.46

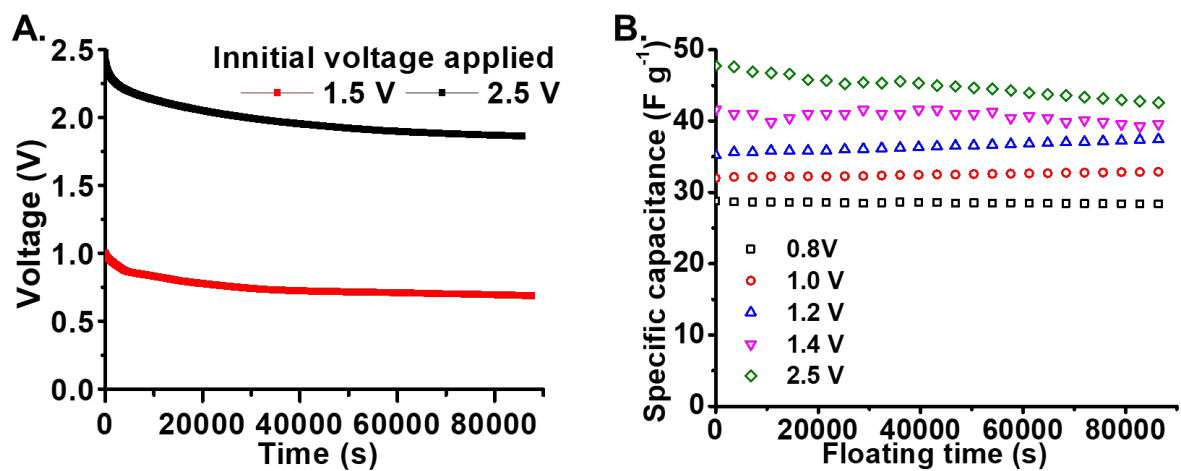


Figure S13. Long term stability analysis. **A.** Self-discharge behavior of asymmetric non-aqueous device at two different charging voltage after 100 cycles. **B.** Effect of floating at different voltage values.